Supplementary Information (SI) for Inorganic Chemistry Frontiers.

Supporting information

Structural optimization of $VO_2/NH_4V_4O_{10}$ cathode materials for high-performance wide-temperature zinc-ion batteries

Ming Zhao[a], Xiang Wu[a,*], Yoshio Bando[b,c,*]

[a]School of Materials Science and Engineering, Shenyang University of Technology, Shenyang 110870, China

[b]Chemistry Department, College of Science, King Saud University, P.O.Box: 2455, Riyadh 11451, Saudi Arabia

[c]Institute for Superconducting and Electronic Materials, University of Wollongong, Squires Way, North Wollongong, NSW 2500, Australia

*E-mail addresses: wuxiang05@sut.edu.cn; BANDO.Yoshio@emeritus.nims.go.jp

1. Experiment section

1.1 Material preparation

Synthesis of Ce-VO/NHVO samples: All the chemicals were utilized without other purification. Firstly, 0.58 g NH_4VO_3 powder were dissolved into 60 ml deionized water at 65 ^oC to form a homogeneous solution. Then, 1.07 g $H_2C_2O_4 \cdot 2H_2O$ were added into the orange solution after 30 min stirring. Subsequently, 0.05 mmol of $Ce(NO_3)_3 \cdot 6H_2O$ were put into the mixture and stirred for another 30 min. The solution was then transferred into an 80 ml Teflon-lined autoclave and maintained at 180 ^oC for 3 h. Finally, the 0.05Ce-VO/NHVO sample were centrifuged several times with deionized water and alcohol then dried in a vacuum oven for 12 h. For comparison, 0, 0.02 and 0.1 mmol of $Ce(NO_3)_3 \cdot 6H_2O$ was applied to synthesize three additional products, named as VO/NHVO, 0.02Ce-VO/NHVO and 0.1Ce-VO/NHVO, respectively.

Preparation of VO_2 nanosheet: In a typical synthesis process, 1.27 g of V_2O_5 powder and 1.77 g of $H_2C_2O_4 \cdot 2H_2O$ sample were dissolved in 40 ml deionized water and stirred at 75 ^oC for 1 h to form a homogeneous solution. Then it was transferred into a Teflon-lined stainless-steel autoclave and heated at 180 ^oC for 3 hours.

Fabrication of $NH_4V_4O_{10}$ material: The obtained $NH_4V_4O_{10}$ sample was synthesized via a hydrothermal route. 0.58 g NH_4VO_3 power was dispersed into 60 ml de-ionized water at 65 ^oC and stirring for half an hour. Subsequently, 0.63 g $H_2C_2O_4 \cdot 2H_2O$ was gradually added to the above solution. The mixture was then reacted in a stainless-steel autoclave at 180 ^oC for 3 h.

1.2 Morphology and structure characterization

X-ray diffraction (XRD) patterns were investigated to study the crystallographic information of the prepared samples (XRD, Shimadzu-7000, Cu Kα radiation, λ = 0.1541 nm). In addition, the surface chemical composition of the products was characterized by X-ray photoelectron spectroscopy (XPS, Thermo Scientific). The morphology and microstructure were conducted by scanning electron microscope (SEM, Gemini 300-71-31) and transmission electron microscope (TEM, JEM-2100 PLUS). Meanwhile, inductively coupled plasma mass spectrometry (ICP-OES, America Agilent 5110) was used to assess the concentration of Ce ion in the prepared materials.

1.3 Electrochemical characterization

Some CR2032-type coin cells were assembled to investigate the electrochemical performance of the samples in air. The cathode was composite of the as-prepared material, carbon black and polyvinylidene fluoride (PVDF) in a weight ratio of 7:2:1. Subsequently, a certain amount of N-methyl-l-2-pyrrolidone (NMP) was poured into the mixture as a dispersant to form a slurry. Then it was evenly coated on a graphite paper and dried in a vacuum oven at 60 ^{o}C for 12 h. The cycling stability and galvanostatic intermittent titration technique (GITT) were characterized by a Neware battery tester (CT-4008T-5V6A-164) within a potential range of 0.2-1.6 V. Additionally, the cyclic voltammetry (CV) curves and electrochemical impedance spectroscopy (EIS) was studied using an electrochemical workstation (CHI660E).

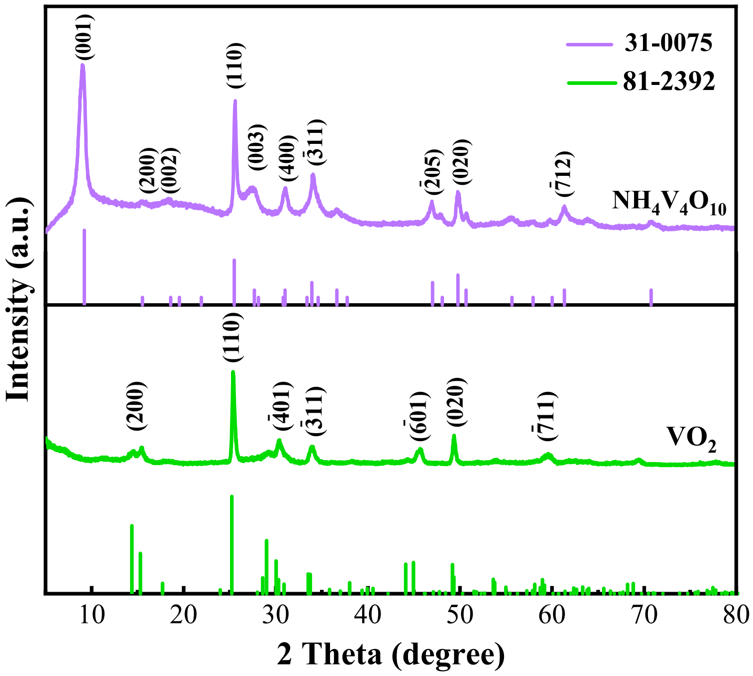

Fig. S1 XRD patterns of the VO_2 and $NH_4V_4O_{10}$ materials

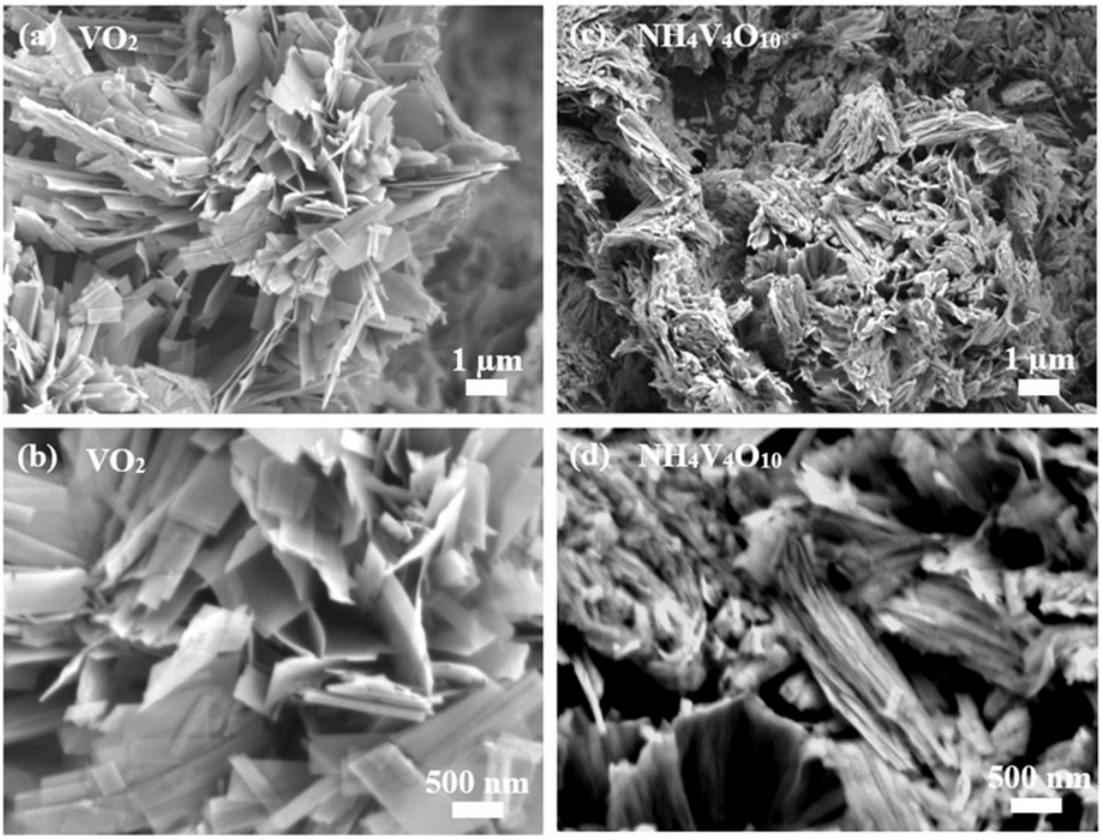

Fig. S2 SEM images (a, b) VO_2 (c, d) $NH_4V_4O_{10}$ samples

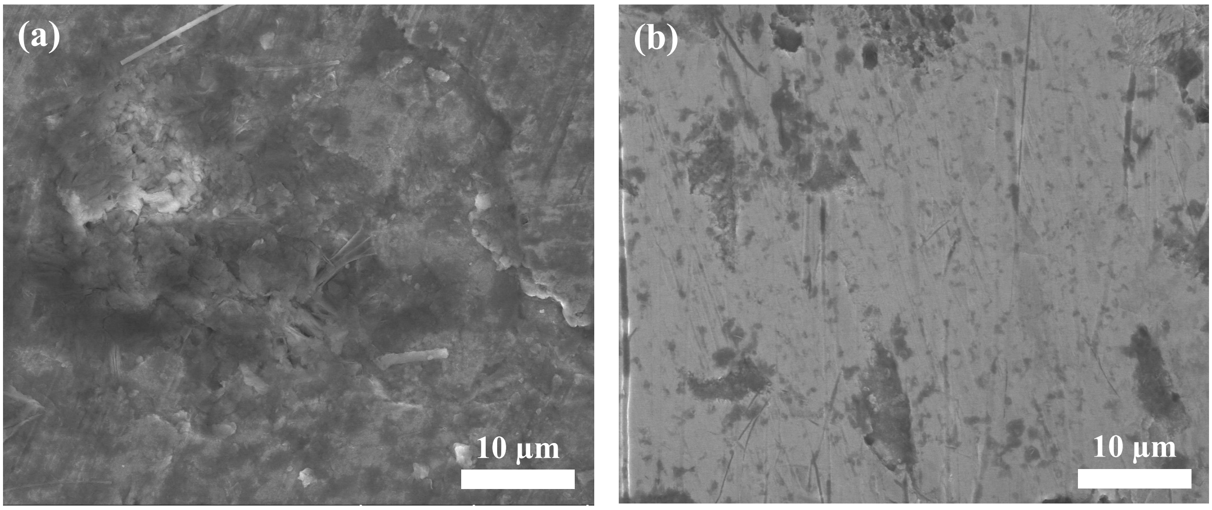

Fig. S3 SEM images of Zn anodes after cycles (a) $Zn(CF_3SO_3)_2$ (b) $Zn(CF_3SO_3)_2$ + Ce^{3+} electrolytes

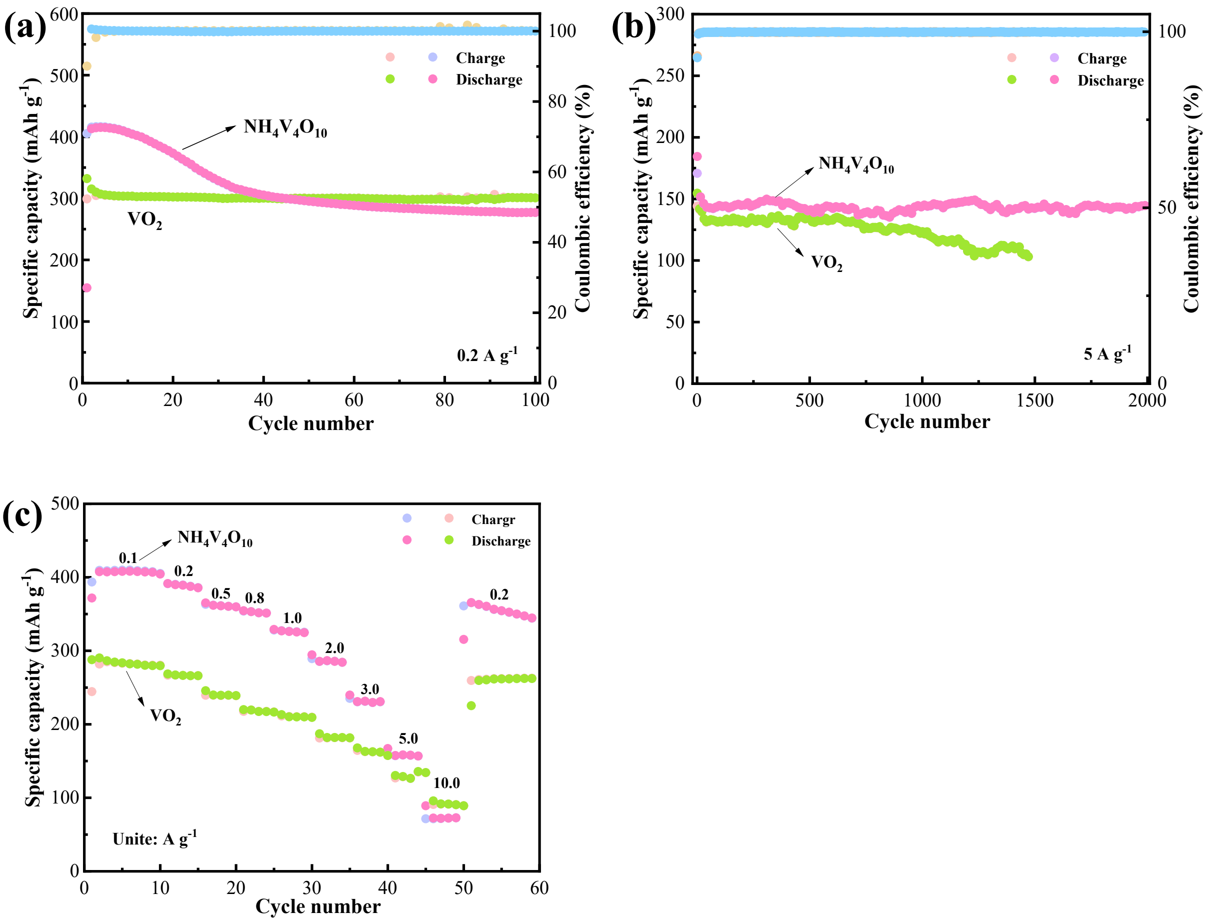

Fig. S4 (a) cycling performance at 0.2 A g^{-1} (b) long-term cycle at 5 A g^{-1} (c) rate performance

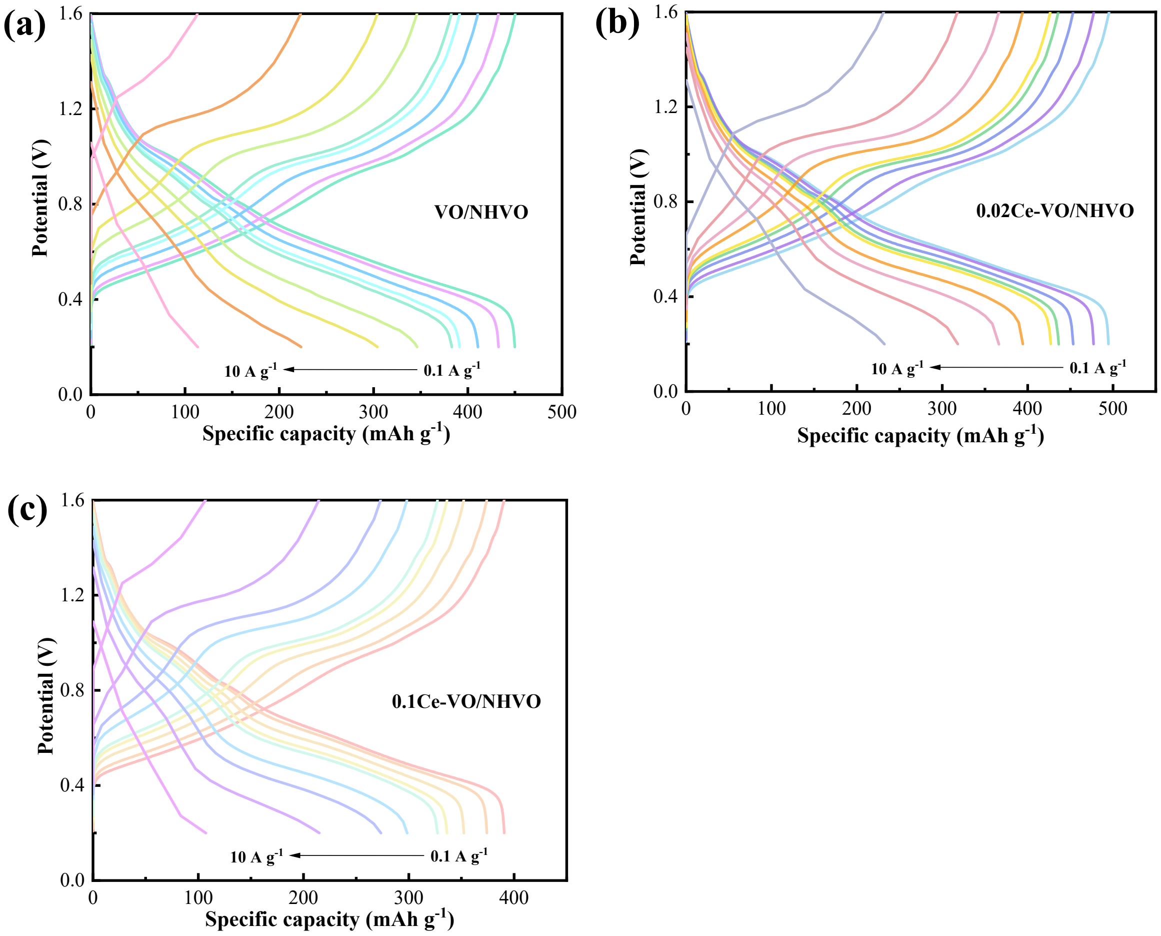

Fig. S5 GCD curves of different samples (a) VO/NHVO (b) 0.02Ce-VO/NHVO (c) 0.1Ce-VO/NHVO

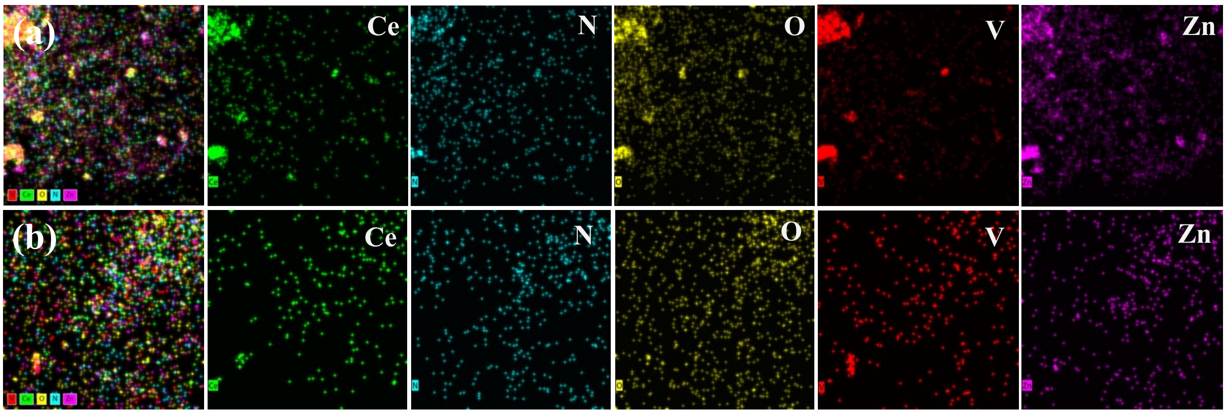

Fig. S6 element mapping image (a) discharging states and (b) charging states